Original Article | Cardiovascular Imaging

https://doi.org/10.3348/kjr.2018.19.6.1031
pISSN 1229-6929 · eISSN 2005-8330
Korean J Radiol 2018;19(6):1031-1041

Korean Journal of Radiology
KJR

Image Quality and Radiation Dose of High-Pitch Dual-Source Spiral Cardiothoracic Computed Tomography in Young Children with Congenital Heart Disease: Comparison of Non-Electrocardiography Synchronization and Prospective Electrocardiography Triggering

Hyun Woo Goo, MD, PhD

Department of Radiology and Research Institute of Radiology, University of Ulsan College of Medicine, Asan Medical Center, Seoul 05505, Korea

Objective: To compare image quality and radiation dose of high-pitch dual-source spiral cardiothoracic computed tomography (CT) between non-electrocardiography (ECG)-synchronized and prospectively ECG-triggered data acquisitions in young children with congenital heart disease.

Materials and Methods: Eighty-six children (≤ 3 years) with congenital heart disease who underwent high-pitch dual-source spiral cardiothoracic CT were included in this retrospective study. They were divided into two groups (n = 43 for each; group 1 with non-ECG-synchronization and group 2 with prospective ECG triggering). Patient-related parameters, radiation dose, and image quality were compared between the two groups.

Results: There were no significant differences in patient-related parameters including age, cross-sectional area, body density, and water-equivalent area between the two groups ($p > 0.05$). Regarding radiation dose parameters, only volume CT dose index values were significantly different between group 1 (1.13 ± 0.09 mGy) and group 2 (1.07 ± 0.12 mGy, $p < 0.02$). Among image quality parameters, significantly higher image noise (3.8 ± 0.7 Hounsfield units [HU] vs. 3.3 ± 0.6 HU, $p < 0.001$), significantly lower signal-to-noise ratio (105.0 ± 28.9 vs. 134.1 ± 44.4, $p = 0.001$) and contrast-to-noise ratio (84.5 ± 27.2 vs. 110.1 ± 43.2, $p = 0.002$), and significantly less diaphragm motion artifacts (3.8 ± 0.5 vs. 3.7 ± 0.4, $p < 0.04$) were found in group 1 compared with group 2. Image quality grades of cardiac structures, coronary arteries, ascending aorta, pulmonary trunk, lung markings, and chest wall showed no significant difference between groups ($p > 0.05$).

Conclusion: In high-pitch dual-source spiral pediatric cardiothoracic CT, additional ECG triggering does not substantially reduce motion artifacts in young children with congenital heart disease.

Keywords: *Cardiothoracic CT; Congenital heart disease; Child; High-pitch dual-source spiral CT; Electrocardiography synchronization*

INTRODUCTION

Cardiothoracic computed tomography (CT) is useful for evaluating congenital heart disease in children, and electrocardiography (ECG)-synchronized CT data acquisition significantly reduces cardiac motion artifacts (1-7). However, respiratory motion artifacts often degrade the image quality of cardiothoracic CT in free-breathing children. The recently introduced high-pitch dual-source spiral CT imaging technique can provide excellent

Received February 5, 2018; accepted after revision May 8, 2018.
Corresponding author: Hyun Woo Goo, MD, PhD, Department of Radiology and Research Institute of Radiology, University of Ulsan College of Medicine, Asan Medical Center, 88 Olympic-ro 43-gil, Songpa-gu, Seoul 05505, Korea.
• Tel: (822) 3010-4388 • Fax: (822) 476-0090 • E-mail: ghw68@hanmail.net

coronary artery image quality in adult patients (8-17) and substantially reduces respiratory motion artifacts in free-breathing patients (14). Two types of scan methods, non-ECG-synchronized and prospectively ECG-triggered methods, are available for high-pitch dual-source spiral CT imaging techniques (8). Prospectively ECG-triggered high-pitch scanning is primarily used for coronary CT angiography because it produces excellent whole heart image quality in a single cardiac cycle (9, 10, 12-17).

High-pitch dual-source spiral CT is highly effective at not only reducing both cardiac and respiratory motion artifacts in free-breathing children, but also at achieving low radiation dose (18-24). Among previous studies, both non-ECG-synchronized high-pitch scanning (18, 23, 24) and prospectively ECG-triggered high-pitch scanning have been utilized (19-22). However, it has not yet been determined whether prospective ECG triggering may add additional value to high-pitch dual-source spiral scanning in free-breathing children, which is particularly crucial in evaluating congenital heart disease. Therefore, this study aimed to compare image quality and radiation dose of free-breathing high-pitch dual-source spiral cardiothoracic CT between non-ECG-synchronized and prospectively ECG triggered data acquisitions in young children with congenital heart disease.

MATERIALS AND METHODS

This retrospective study was approved by the local Institutional Review Board and informed consent was waived.

Study Population

Between October 2010 and November 2016, 3127 pediatric cardiothoracic CT examinations were performed. Among these, 509 CT studies (16.3%) were acquired with high-pitch dual-source spiral scanning (357 studies using non-ECG synchronized scanning and 152 studies using prospectively ECG-triggered scanning). Exclusion criteria included patients older than 3 years of age, the use of tube voltages other than 80 kV (n = 14 for 70 kV, n = 2 for 100 kV in patients younger than 3 years of age), previous history of severe side effects from iodinated contrast agent, and severe renal failure. Finally, 86 children with congenital heart disease who underwent free-breathing high-pitch dual-source spiral cardiothoracic CT at 80 kV were included in the study and divided into two age, sex, and body size-matched groups (n = 43 for each; group 1 for non-ECG-synchronization and group 2 for prospective ECG triggering) to compare image quality and radiation dose (Table 1).

Congenital heart diseases in group 1 were as follows: 17 cases of functional single ventricle, 11 coarctation of the aorta, three pulmonary atresia with ventricular septal defect (VSD), two VSD, two double outlet right ventricle, two interrupted aortic arch, two anomalous pulmonary venous return, two atrial septal defect, one aberrant left subclavian artery, one truncus arteriosus, and one pulmonary atresia with intact ventricular septum. While those in group 2 comprised: 22 case of functional single ventricle, three double outlet right ventricle, three anomalous pulmonary venous return, two coarctation of the aorta, two VSD, two pulmonary atresia with VSD, two pulmonary atresia with intact ventricular septum, two aberrant left subclavian

Table 1. Patient Characteristics and Radiation Dose of High-Pitch Dual-Source Pediatric Cardiothoracic CT in Two Groups

	Group 1 (n = 43)	Group 2 (n = 43)	*P*
Male:female	26:17	26:17	NA
Age (months)	Median 6.0 (range 1 day–3 years); 8.4 ± 8.4	Median 6.0 (range 1 day–3 years); 8.4 ± 8.6	0.993
Heart rate (beats per minute)	NA	Median 119 (range 86–169); 123.0 ± 19.2	NA
Heart rate variability (beats per minute)	NA	Median 9 (range 2–247); 64.0 ± 15.6	NA
Cardiac phase error	NA	8/43 (18.6%)	NA
Cross-sectional area (cm^2)	156.7 ± 26.7	158.1 ± 35.2	0.837
Body density (HU)	-209.0 ± 52.8	-208.9 ± 48.1	0.994
A_w (cm^2)	123.6 ± 20.3	124.4 ± 25.4	0.848
Volume CT dose index (mGy)	1.13 ± 0.09	1.07 ± 0.12	0.017
Dose-length product (mGy·cm)	17.8 ± 3.4	17.0 ± 3.7	0.252
Effective dose (mSv)	0.8 ± 0.3	0.8 ± 0.3	0.390
Scan range (cm)	15.7 ± 2.0	15.7 ± 1.8	0.882
Tube current modulation	25/43 (58.1%)	43/43 (100.0%)	NA

A_w = water-equivalent area, CT = computed tomography, HU = Hounsfield units, NA = not applicable

Korean Journal of Radiology
KJR

artery, one tetralogy of Fallot, one atrioventricular septal defect, one congenitally-corrected transposition of the great arteries, one patient ductus arteriosus, and one sinus of Valsalva aneurysm. Reasons for cardiothoracic CT examination in the two groups are summarized in Table 2.

High-Pitch Dual-Source Spiral Cardiothoracic CT

High-pitch dual-source spiral cardiothoracic CT was performed using a 128-slice dual-source scanner (SOMATOM Definition Flash; Siemens Healthineers, Forchheim, Germany) with 2 x 64 x 0.6 mm slices using the z-flying focal spot technique, a gantry rotation time of 280 msec, a temporal resolution of 75 msec, a 0.75-mm slice width, and a 0.4-mm reconstruction interval during free-breathing in all patients. In our institution, the high-pitch dual-source spiral scan mode is mainly utilized, if the assessment of coronary artery anatomy or ventricular function is not critical or when a patient is so clinically unstable they need an ultrafast scanning technique. For patient sedation, oral choral hydrate (50 mg/kg) was initially administered with additional intravenous midazolam (0.1 mg/kg) or ketamine (1 mg/kg) as required.

In January 2013, the scan mode of high-pitch dual-source spiral cardiothoracic CT was changed from non-

Table 2. Reasons for Cardiothoracic CT Examinations in Two Groups

Group 1 (n = 43)	Group 2 (n = 43)
Pulmonary vascular morphology and/or ventricular outflow dimensions and/or conduit/shunt patency in repaired functional single ventricle (n = 15)	Pulmonary vascular morphology and/or ventricular outflow dimensions and/or conduit/shunt patency in repaired functional single ventricle (n = 18)
Follow-up after aortic arch repair in coarctation of aorta (n = 6)	Cardiovascular morphology of unrepaired functional single ventricle (n = 4)
Initial work-up of coarctation of aorta (n = 4)	Pulmonary vascular morphology and/or ventricular outflow dimensions and/or airway in repaired double outlet right ventricle (n = 3)
Mapping of major aortopulmonary collateral arteries (n = 3)	Pulmonary vein morphology in repaired total anomalous pulmonary venous return (n = 3)
Follow-up after aortic arch repair in interrupted aortic arch (n = 2)	Cardiovascular morphology in repaired pulmonary atresia with intact ventricular septum (n = 2)
Pulmonary vascular morphology and/or ventricular outflow dimensions in repaired double outlet right ventricle (n = 1)	Initial work-up of coarctation of aorta (n = 2)
Pulmonary vascular morphology in unrepaired double outlet right ventricle (n = 1)	Postoperative complications in repaired pulmonary atresia with VSD (n = 2)
Follow-up of vascular airway compression after aortopexy in repaired coarctation of aorta (n = 1)	Cardiovascular morphology of unrepaired congenitally corrected transposition of great arteries (n = 1)
Suspected aortic arch obstruction after atrial septal defect closure (n = 1)	Left pulmonary artery stenosis in unrepaired VSD (n = 1)
Morphology of unrepaired muscular VSDs (n = 1)	Right pulmonary artery stenosis after patent ductus arteriosus ligation (n = 1)
Airway in unrepaired VSD (n = 1)	Suspected aberrant left subclavian artery (n = 1)
Aortic arch and airway in repaired functional single ventricle (n = 1)	Cardiovascular morphology in repaired VSD (n = 1)
Suspected partial anomalous pulmonary venous return (n = 1)	Initial work-up of sinus of Valsalva aneurysm (n = 1)
Pulmonary vein morphology in repaired total anomalous pulmonary venous return (n = 1)	Follow-up after repaired aberrant left subclavian artery (n = 1)
Follow-up after repaired aberrant left subclavian artery (n = 1)	Preoperative evaluation in unrepaired tetralogy of Fallot (n = 1)
Pulmonary vascular morphology and collateral vessels in repaired pulmonary atresia with intact ventricular septum (n = 1)	Suspected left pulmonary artery sling in unrepaired atrioventricular septal defect (n = 1)
Cardiovascular morphology of unrepaired functional single ventricle (n = 1)	
Cardiovascular morphology and airway in repaired truncus arteriosus (n = 1)	

VSD = ventricular septal defect

ECG-synchronized data acquisition to prospectively ECG-triggered data acquisition, expecting an additional benefit of the latter in free-breathing young children. Non-ECG-synchronized scanning was obtained with pitch 3.2 in group 1 and prospectively ECG-triggered scanning was acquired with pitch 3.4 in group 2. In group 1, caudocranial CT scan direction was used to minimize perivenous streak artifacts resulting from undiluted contrast agent. In group 2, craniocaudal or caudocranial CT scan direction was used to adjust the scan range during the end-systolic phase on the ECG in the conotruncal region of the heart for each patient. Since their heart rates exceeded 75 beats per minutes, the end-systolic cardiac phase rather than mid-diastolic phase was used in all patients by targeting the second half of the T wave on ECG as previously described (2, 9). ECG electrodes were placed in regions far away from the scan range, such as on the shoulder, arms, and abdomen to avoid streak artifact from the metallic electrodes (Fig. 1). Cardiac phase error was defined to be present when the R wave on ECG was included in a scan period or the second half of the T wave was not included in a scan period (Fig. 2). In group 2, average heart rates during CT examination were recorded and heart rate variability was calculated by subtracting minimal heart rate from maximal heart rate during CT examination. However, heart rates were not available in group 1 without ECG records during CT examination and therefore could not be compared between the two groups.

To obtain uniform image noise, a volume CT dose index value based on a 32-cm phantom was individually determined. This was based on the cross-sectional area and mean body density measured on an axial CT image obtained approximately 1–2 cm above the dome of the liver for bolus

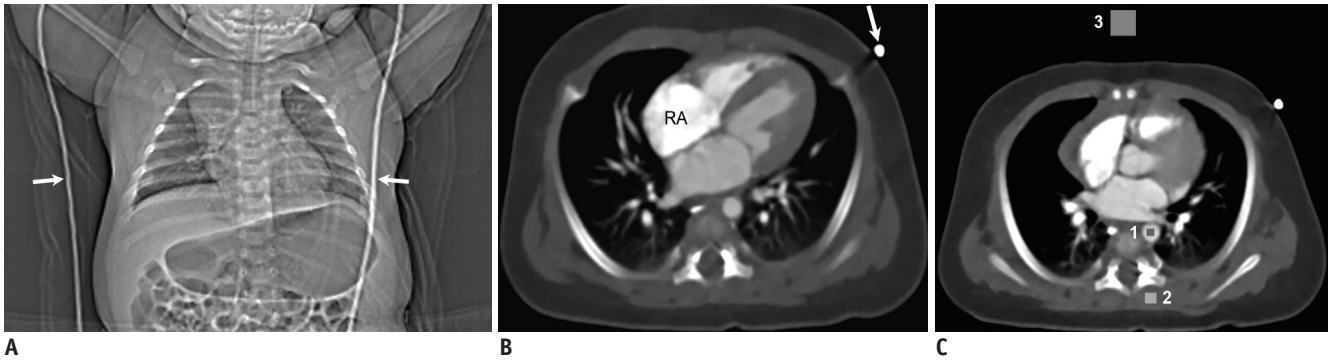

Fig. 1. 77-day-old boy with coarctation of aorta.
A. CT scout image shows ECG cables (arrows) for prospective ECG triggering. ECG electrodes placed on both arms are not shown on CT scout image. **B.** Axial CT image showing left-side ECG cable (arrow) causing mild streak artifact. Mild streak artifacts also are shown around RA. As result, degree of streak artifacts was assessed as grade 3 indicating mildly degraded image quality. **C.** Axial CT image at level of aortic sinus shows locations of three rectangular regions of interest for measuring CT densities in descending aorta (1), paraspinal muscle (2), and air (3). CT = computed tomography, ECG = electrocardiography, RA = right atrium

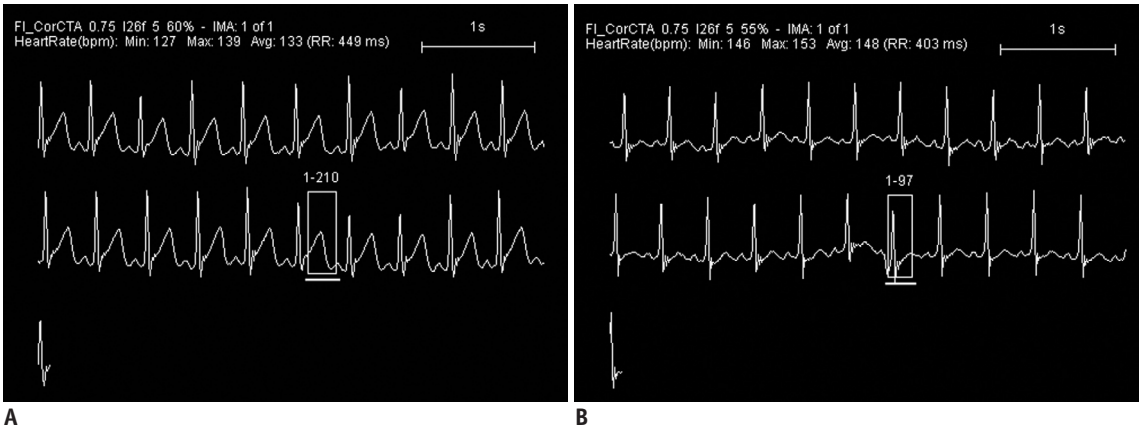

Fig. 2. Scan period positions in prospectively ECG-triggered high-pitch dual-source cardiothoracic CT scanning on ECG.
A. In 77-day-old boy with coarctation of aorta and cervical aortic arch, scanning period on ECG, indicated by rectangle, is optimally located, starting from T wave and finishing with P wave peak. **B.** In contrast, scanning period on ECG, indicated by rectangle, is poorly positioned, overlapping with R wave in 13-day-old boy with hypoplastic left heart syndrome.

Korean Journal of Radiology
KJR

tracking (25). Patient diameter or area is often used to reflect patient body size. However, body density should be incorporated into these indices in order to avoid substantial errors especially in the thoracic region (26). Consequently, water-equivalent diameter or area may be used to indicate patient body size with high fidelity and can be utilized in CT radiation dose optimization. Water-equivalent area (A_w) was calculated from the measured cross-sectional area (A_{body}) and mean body density (D_{body}) of each patient by using the following formula:

$$A_w = (D_{body} / 1000 + 1) \times A_{body} \quad (1)$$

An adaptive section collimator was used to reduce additional radiation exposure due to z-overscanning in both groups as described in previous studies (8, 18). Combined tube current modulation (CARE Dose 4D; Siemens Healthineers) was not always used because its dose-saving effect was disputable in the high pitch value (3.2) in group 1; while it was used in all patients despite the high pitch value (3.4) in group 2 expecting an additional dose-saving effect (Table 1).

In addition to thin-section axial CT images, 2- or 3 mm-thick axial, coronal, sagittal, and oblique reformatted CT images were reconstructed. For image reconstruction, the sinogram-affirmed iterative reconstruction (SAFIRE; Siemens Healthineers) strength 5 with a medium smooth kernel (I26f) was used. Iodinated contrast agent (Iomeron [iomeprol] 400, 400 mg I/mL; Bracco Imaging SpA, Milan, Italy; 1.5–2.0 mL/kg) was intravenously administered at an injection rate of 0.2–1.0 mL/s using a dual-head power injector and a tri-phasic injection protocol, in which undiluted contrast agent was followed by 50% diluted contrast agent and then by 5% diluted contrast agent. This was performed to achieve uniform cardiovascular enhancement and minimal perivenous streak artifacts from undiluted contrast agent. More specifically, the first, second, and third parts of the tri-phasic protocol contribute to optimal systemic arterial and left heart, pulmonary vascular and right heart, and systemic venous enhancements, respectively. The scan delay time was determined by a bolus tracking technique with a trigger threshold of 150 Hounsfield units (HU) in the left ventricular cavity.

Comparison of CT Radiation Dose

The volume CT dose index and dose-length product values based on a 32-cm phantom of cardiothoracic CT displayed on the patient protocol were recorded. Effective dose values of cardiothoracic CT were calculated by multiplying the dose-length product with patient age and gender, and tube voltage-specific conversion factors for chest CT (27).

Quantitative Evaluation of CT Image Quality

On axial CT images at the level of the aortic valve sinus, CT density was measured in the descending aorta, paraspinal muscle, and air by placing rectangular regions of interest in the areas showing homogeneous attenuation (Fig. 1C). In particular, a lung window setting was used to avoid the interference of patient clothes and blanket in the measurement of air density. Although the same tube voltage (80 kVp) was used in all cardiothoracic CT scans, standard deviations of aortic and muscular densities might be affected by a different level of contrast enhancement. Therefore, the standard deviation of air density was used for image noise on the CT images. Since a 2- or 3-mm slice thickness (S) was used to reconstruct thick-section axial CT images, the image noise (σ) was normalized to a slice thickness of 3 mm using the following formula:

$$\sigma^2 \propto 1/S \quad (2)$$

From aortic density (D_{aorta}) and slice thickness-normalized image noise from air density (σ_{air}), signal-to-noise ratio (SNR) was calculated using the following formula:

$$SNR = D_{aorta} / \sigma_{air} \quad (3)$$

From mean aortic density (D_{aorta}), muscle density (D_{muscle}), and slice thickness-normalized image noise from air density (σ_{air}), contrast-to-noise ratio (CNR) was calculated using the following formula:

$$CNR = (D_{aorta} - D_{muscle}) / \sigma_{air} \quad (4)$$

Subjective Evaluation of CT Image Quality

Subjective CT image quality was assessed by a pediatric radiologist with 17 years of experience in pediatric cardiothoracic CT. Motion artifact grade on axial, coronal, sagittal, and oblique reformatted CT images was evaluated for the cardiac structures, coronary arteries, ascending aorta, pulmonary trunk, lung markings, diaphragm, and chest wall using a 4-point scale (grade 1, severely degraded; grade 2, moderately degraded; grade 3, mildly degraded; and grade 4, excellent, no artifact). In addition,

the grade of streak artifacts, including those resulting from ECG electrodes on axial, coronal, and sagittal CT images was assessed using the same 4-point scale. Motion artifacts in the lung markings were evaluated using the lung window setting while others were evaluated using the mediastinal window setting. To evaluate intra-observer variability in subjective image quality grading, the second session of the evaluation was repeated 6 months after the first session and these two values then were averaged. The overall grade was subsequently calculated as the average of these eight grades for each patient.

Statistical Analysis

For statistical analysis, the statistical software SPSS (version 24.0; IBM Corp., Armonk, NY, USA) was used. Continuous or ordinal variables are presented as mean ± standard deviation or median with range, and categorical variables are expressed as frequency with percentage. Unpaired *t* test and Mann-Whitney U test were used to compare the difference between two means of continuous and ordinal variables, respectively, between the two groups. In group 2, subjective image quality was compared between two subgroups, with and without cardiac phase error. Intra-observer agreement on subjective image quality of high-pitch dual-source spiral cardiothoracic CT was evaluated using Cohen's kappa statistics. A *p* value of less than 0.05 was considered to be statistically significant.

RESULTS

Patient Characteristics

Patient characteristics in the two groups are described in Table 1. No significant differences in age (8.4 ± 8.4 months vs. 8.4 ± 8.6 months, $p = 0.993$), cross-sectional area (156.7 ± 26.7 cm^2 vs. 158.1 ± 35.2 cm^2, $p = 0.837$), body density (-209.0 ± 52.8 HU vs. -208.9 ± 48.1 HU, $p = 0.994$), and A_w (123.6 ± 20.3 cm^2 vs. 124.4 ± 25.4 cm^2, $p = 0.848$) were found between group 1 and group 2, respectively (Table 1). In group 2, average heart rate and heart rate variability during CT examination were 123.0 ± 19.2 beats per minute and 17 ± 38 beats per minute, respectively. Erroneous selection of cardiac phases in prospective ECG triggering occurred in eight out of 43 patients (18.6%) in group 2.

CT Radiation Dose

CT radiation dose parameters in the two groups are summarized in Table 1. No significant differences in dose-length product (17.8 ± 3.4 mGy·cm vs. 17.0 ± 3.7 mGy·cm, $p = 0.252$), effective dose (0.8 ± 0.3 mSv vs. 0.8 ± 0.3 mSv, $p = 0.390$), and scan range (15.7 ± 2.0 cm vs. 15.7 ± 1.8 cm, $p = 0.882$) were found between group 1 and group 2, respectively (Table 1). In contrast, volume CT dose index values of group 1 (1.13 ± 0.09 mGy) were significantly higher than those of group 2 (1.07 ± 0.12 mGy, $p = 0.017$) (Table 1). Combined tube current modulation was used in 25 out of 43 patients (58.1%) in group 1 and in all patients in group 2 (Table 1).

Quantitative Image Quality

Quantitative image quality parameters in the two groups are described in Table 3. There were no significant differences in the measured CT densities in the descending aorta (398.2 ± 117.3 HU vs. 429.6 ± 126.3 HU, $p = 0.240$), paraspinal muscle (76.8 ± 11.6 HU vs. 76.5 ± 12.0 HU, $p = 0.910$), or air (-984.0 ± 27.6 HU vs. -987.6 ± 23.4 HU, $p = 0.650$) between group 1 and group 2, respectively (Table 3). In contrast, significantly higher image noise (3.8 ± 0.7 HU vs. 3.3 ± 0.6 HU, $p < 0.001$), and significantly lower SNR (105.0 ± 28.9 vs. 134.1 ± 44.4, $p = 0.001$) and contrast noise-to-ratio (84.5 ± 27.2 vs. 110.1 ± 43.2, $p = 0.002$) were found in group 1 compared with group 2 (Table 3).

Subjective Image Quality

Subjective image quality parameters in the two groups are summarized in Table 4. There were no significant differences in overall grades (3.5 ± 0.6 vs. 3.5 ± 0.6, $p = 0.574$), cardiac motion grades (3.4 ± 0.5 vs. 3.5 ± 0.5, $p = 0.361$), coronary artery motion grades (3.0 ± 0.8 vs. 3.2 ±

Table 3. Quantitative Image Quality Evaluation of High-Pitch Dual-Source Pediatric Cardiothoracic CT in Two Groups

	Group 1 (n = 43)	Group 2 (n = 43)	*P*
CT density of descending aorta (HU)	398.2 ± 117.3	429.6 ± 126.3	0.240
CT density of paraspinal muscle (HU)	76.8 ± 11.6	76.5 ± 12.0	0.910
CT density of air (HU)	-984.0 ± 27.6	-987.6 ± 23.4	0.650
Image noise (HU)	3.8 ± 0.7	3.3 ± 0.6	< 0.001
Signal-to-noise ratio	105.0 ± 28.9	134.1 ± 44.4	0.001
Contrast-to-noise ratio	84.5 ± 27.2	110.1 ± 43.2	0.002

Korean Journal of Radiology
KJR

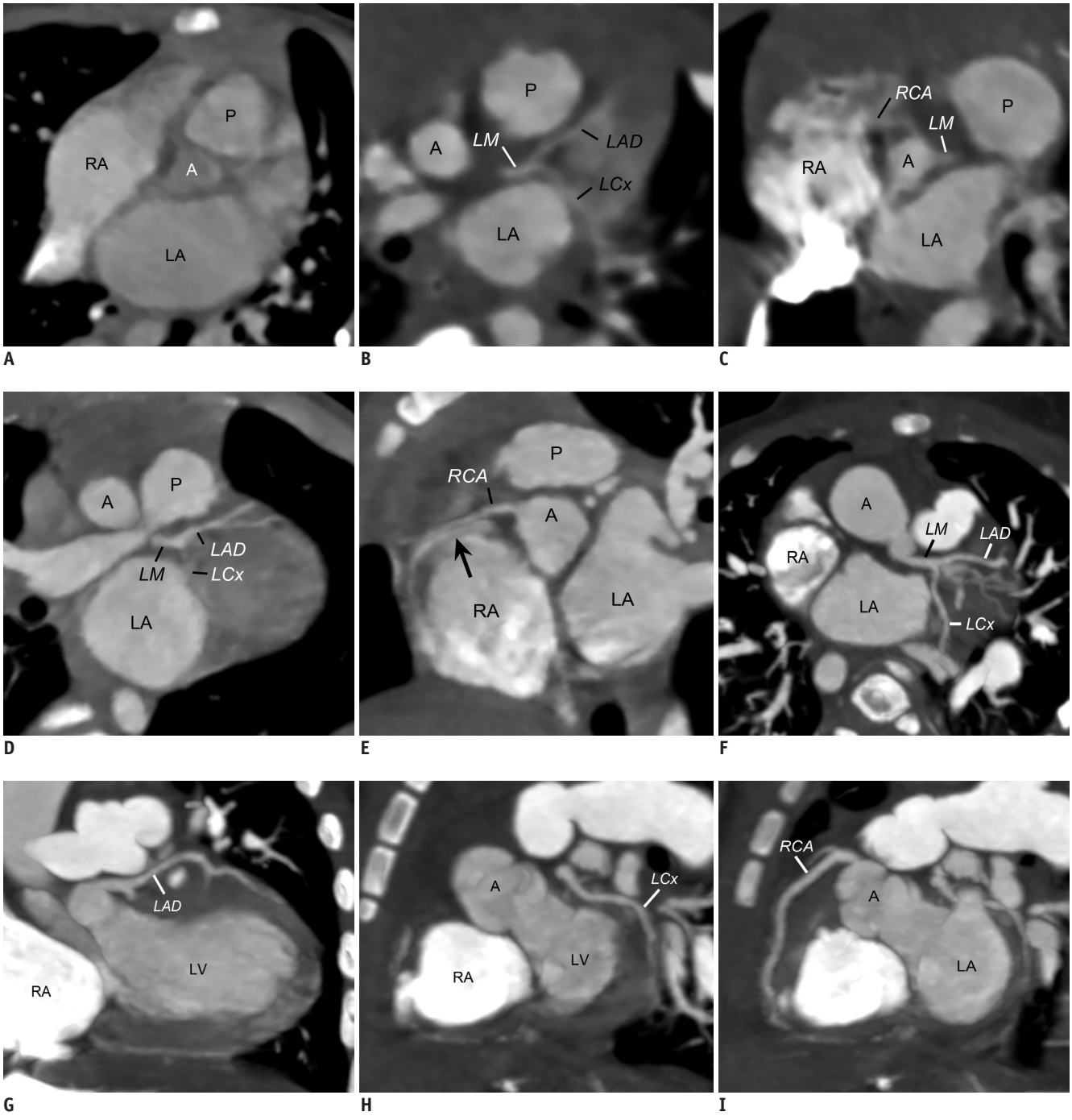

Fig. 3. Coronary artery motion artifact grading of high-pitch dual-source cardiothoracic CT.
A. Oblique coronal CT image acquired with prospective ECG triggering in 35-day-old boy with coarctation of aorta demonstrates severe motion artifacts on coronary arteries that corresponded to grade 1. Oblique CT images **(B, C)** acquired without ECG synchronization in 1-day-old girl with coarctation of aorta illustrate moderate motion artifacts on coronary arteries, especially right coronary artery, which correspond to grade 2. Oblique CT images **(D, E)** acquired without ECG synchronization in an 11-month-old boy with surgically closed atrial septal defect reveal mild motion artifacts (grade 3), especially on right coronary artery, including doubling artifact (arrow) at proximal segment. Oblique CT images (**F-I)** acquired without ECG synchronization in 6-month-old boy with double-outlet right ventricle show no motion artifacts on coronary arteries including left main artery, left anterior descending artery, left circumflex artery, and right coronary artery that corresponded to grade 4. A = ascending aorta, LA = left atrium, LAD = left anterior descending artery, LCx = left circumflex artery, LM = left main artery, LV = left ventricle, P = pulmonary trunk, RCA = right coronary artery

0.8, $p = 0.069$) (Fig. 3), ascending aorta motion grades (3.7 ± 0.5 vs. 3.7 ± 0.6, $p = 0.666$), pulmonary trunk motion grades (3.7 ± 0.4 vs. 3.6 ± 0.5, $p = 0.883$), motion grades in lung markings (3.4 ± 0.5 vs. 3.4 ± 0.6, $p = 0.993$) (Fig. 4), chest wall motion grades (4.0 ± 0.1 vs. 4.0 ± 0.0, $p = 0.317$), or grades of streak artifacts (2.9 ± 0.7 vs. 2.9 ± 0.7, $p = 0.875$) between group 1 and group 2, respectively (Table 4). In contrast, diaphragm motion was significantly less in group 1 (3.8 ± 0.5) than in group 2 (3.7 ± 0.4, $p = 0.036$) (Table 4, Fig. 4). In group 2, streak artifacts from the ECG electrodes for prospective ECG triggering was shown in only one patient (2.3%, 1/43). In contrast, the ECG electrodes placed on the patient's back in admission wards infrequently caused streak artifacts in both groups. Cohen's kappa coefficient was 0.63 ($p < 0.001$) indicating a good intra-observer agreement.

In the subgroup analysis of group 2, cardiac phase error significant degraded not only overall image quality, but also the image quality of the cardiac structures, coronary arteries, and ascending aorta (Table 5).

DISCUSSION

This study demonstrated that image quality and radiation dose of free-breathing high-pitch dual-source spiral pediatric cardiothoracic CT were comparable between non-ECG synchronized scans and prospectively ECG-triggered scans. This finding is in accordance with previous studies comparing between non-ECG-synchronized and prospectively ECG-triggered scan modes of high-pitch dual-source spiral CT of the aorta in adults (28, 29). The two scan modes showed comparable subjective and objective image quality of the aorta, including the aortic root and coronary arteries, as well as radiation dose (28, 29). Consequently, prospective ECG triggering does not add a substantial diagnostic gain to free-breathing high-pitch dual-source spiral cardiothoracic CT in children with congenital heart disease and an additional workflow required for ECG electrode placement

Table 4. Subjective Image Quality Evaluation of High-Pitch Dual-Source Pediatric Cardiothoracic CT in Two Groups

	Group 1 (n = 43)	Group 2 (n = 43)	*P*
Overall grades	3.5 ± 0.6	3.5 ± 0.6	0.574
1. Cardiac motion artifacts	3.4 ± 0.5	3.5 ± 0.5	0.361
2. Motion artifacts in coronary artery	3.0 ± 0.8	3.2 ± 0.8	0.069
3. Motion artifacts in ascending aorta	3.7 ± 0.5	3.7 ± 0.6	0.666
4. Motion artifacts in pulmonary trunk*	3.7 ± 0.4	3.6 ± 0.5	0.883
5. Motion artifacts in lung markings	3.4 ± 0.5	3.4 ± 0.6	0.993
6. Motion artifacts in diaphragm	3.8 ± 0.5	3.7 ± 0.4	0.036
7. Motion artifacts in chest wall	4.0 ± 0.1	4.0 ± 0.0	0.317
8. Streak artifacts†	2.9 ± 0.7	2.9 ± 0.7	0.875

*In evaluating pulmonary trunk, there were four missing data in group 1 and eight missing data in group 2 due to no visible pulmonary trunk on cardiothoracic CT, †Streak artifacts from ECG electrodes were included in group 2. ECG = electrocardiography

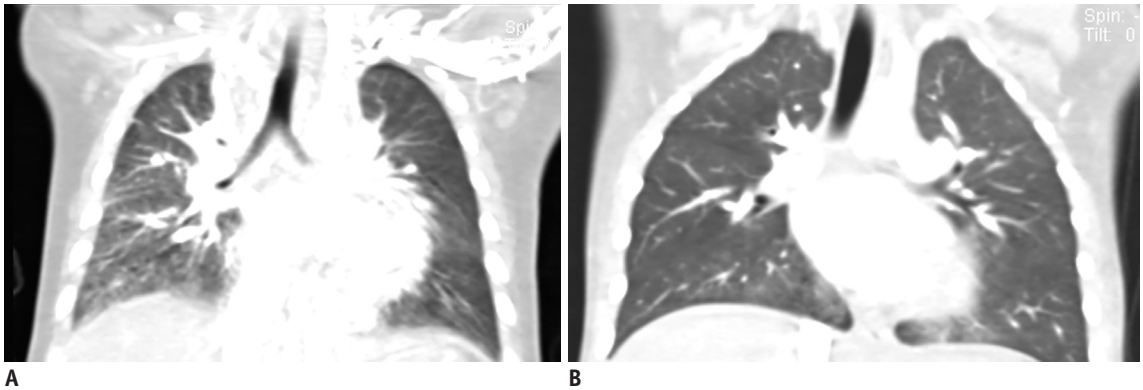

A B

Fig. 4. Lung window setting CT images illustrating motion artifacts in lung markings and diaphragms.
A. Coronal CT image acquired without ECG synchronization in 6-month-old boy with functional single ventricle shows moderate degrees of motion artifacts (grade 2) in lung markings as well as in diaphragm. **B.** Coronal CT image acquired without ECG synchronization in 3-year-old boy with repaired coarctation of aorta displays no motion artifacts (grade 4) in lung markings as well as diaphragm.

Korean Journal of Radiology
KJR

Table 5. Effect of Cardiac Phase Error on Subjective Image Quality in Group 2

	No Error (n = 35)	Error (n = 8)	*P*
Overall grades	3.5 ± 0.6	3.0 ± 0.8	< 0.001
1. Cardiac motion artifacts	3.6 ± 0.4	2.9 ± 0.5	0.001
2. Motion artifacts in coronary artery	3.4 ± 0.6	2.4 ± 1.0	0.003
3. Motion artifacts in ascending aorta	3.9 ± 0.3	2.9 ± 0.8	0.003
4. Motion artifacts in pulmonary trunk*	3.7 ± 0.4	3.3 ± 0.7	0.122
5. Motion artifacts in lung markings	3.4 ± 0.6	3.3 ± 0.7	0.657
6. Motion artifacts in diaphragm	3.7 ± 0.4	3.6 ± 0.5	0.748
7. Motion artifacts in chest wall	4.0 ± 0.0	4.0 ± 0.0	1.0
8. Streak artifacts†	2.9 ± 0.7	2.8 ± 0.7	0.702

*In evaluating pulmonary trunk, there were eight missing data in cases without cardiac phase error due to no visible pulmonary trunk on cardiothoracic CT, †Streak artifacts from ECG electrodes were included.

may therefore be omitted.

The finding of equivalent dose-length product and effective dose between the two scan modes appears to be reliable because patient-related parameters, such as age, sex, A_{boody}, D_{body}, and A_w, potentially influencing CT radiation dose, were strictly matched between the two groups. In contrast, volume CT dose index values in group 1 were significantly higher than those in group 2, probably due to less frequent use of tube current modulation. Unless tube current modulation was not utilized in both groups, radiation dose may be equal between the two. Despite significantly lower volume CT dose index values in group 2, σ was significantly lower in group 2 than in group 1. The result clearly highlights the usefulness of tube current modulation in radiation dose optimization. The combination of slightly higher aortic enhancement and significantly lower σ in group 2 led to significantly higher SNR and CNR in group 2 than in group 1.

Substantial reductions in respiratory motion artifacts on high-pitch dual-source spiral CT have been already reported in both clinical and phantom studies (18, 30). In this study, motion artifacts other than the diaphragm showed no significant difference between the two scan modes. It remains unclear why a small but significant difference in diaphragm motion artifacts was observed between the two groups. It is noteworthy that cardiac phases along the z-axis are different in high-pitch dual-source spiral CT (8). Therefore, scan mode cannot be used for ventricular function assessment (31, 32). In addition, image quality of the coronary arteries tends to be suboptimal at high heart rates (8), which are common in children with congenital heart disease. As a result, the sequential CT scan mode with combined respiratory and ECG triggering is used for pediatric cardiothoracic CT in our institution, when the evaluation of ventricular function and coronary artery anatomy is essential (33).

A previous study reported that streak artifacts resulting from ECG electrodes deteriorate image quality of prospectively ECG-triggered high-pitch dual-source spiral CT (24). In this study, streak artifacts resulting from ECG electrodes could be avoided in almost all patients by placing ECG electrodes outside the longitudinal scan range. As a result, no significant difference in streak artifacts was found between the two scan modes. In contrast, mild streak artifacts from undiluted contrast agent were observed in both groups despite the utilization of the tri-phasic intravenous injection protocol in this study. In high-pitch dual-source spiral CT, the scan delay for optimal contrast enhancement should be adjusted so that its duration is sufficient to compensate for an exceedingly short scan time (34).

In high-pitch dual-source spiral scanning, the use of low tube voltage may result in high image noise due to tube current saturation (8). In fact, this technical limitation often precludes the use of 70 kV for high-pitch dual-source spiral scanning even in small children. To obtain the full advantages of 70 kV in high-pitch dual-source spiral pediatric cardiothoracic CT, a higher radiation dose efficiency is required using improved detector technology and iterative reconstruction algorithm, as well as a stronger X-ray tube. For the same reason, automatic tube voltage selection software leads to higher radiation dose in non-ECG-synchronized high-pitch dual-source spiral CT of the aorta by escalating tube voltage from 100 kV to 120 kV in 80% of patients; this contradicts previous results of automatic tube voltage selection software using standard-pitch single-source scan (35).

This study has several limitations. First, two groups of 43 different patients with different utilized CT scan modes

were compared rather than paired examinations in the same patients due to the retrospective nature of this study. However, patient age, sex, and body size of the two groups were matched to increase the significance of the unpaired comparison. Second, the use of tube current modulation during CT scanning was not completely equal between the two groups. This is because its dose-saving effect during high-pitch dual-source spiral scanning was questionable at that time. Nonetheless, an additional dose-saving effect of tube current modulation was proven for high-pitch dual-source spiral scanning even with a relatively short scan range, approximately 16 cm. Third, the degree of respiratory motion, such as respiratory rate or respiratory excursion, between the two groups could not be controlled in this retrospective study, and there were unexpectedly less diaphragm motion artifacts in group 1 compared with group 2. Nonetheless, the results may at least suggest non-inferiority of the non-ECG-synchronized scan mode in reducing respiratory motion artifacts, compared with the prospectively ECG-triggered scan mode. Fourth, the pitches of the two scans were slightly different: 3.2 for non-ECG-synchronized high-pitch dual-source spiral scanning and 3.4 for prospectively ECG-triggered high-pitch dual-source spiral scanning. These values were selected because they are the maximal values for each scan and were expected to show the most beneficial effects in reducing motion artifacts. They were different due to the retrospective nature of this study. However, a 0.2 difference in pitch might not substantially affect the results of this study. Fifth, inter-observer agreement was not evaluated in this study. However, intra-observer agreement was evaluated as in a previous study (29). Sixth, diagnostic accuracy was not compared because it was beyond the scope of the study.

In conclusion, additional ECG triggering does not substantially reduce motion artifacts on high-pitch dual-source spiral pediatric cardiothoracic CT in young children with congenital heart disease. In high-pitch dual-source spiral cardiothoracic CT, the use of tube current modulation appears to reduce radiation dose.

REFERENCES

1. Goo HW, Park IS, Ko JK, Kim YH, Seo DM, Yun TJ, et al. CT of congenital heart disease: normal anatomy and typical pathologic conditions. *Radiographics* 2003;23 Spec No:S147-S165
2. Goo HW. State-of-the-art CT imaging techniques for congenital heart disease. *Korean J Radiol* 2010;11:4-18
3. Goo HW, Yang DH. Coronary artery visibility in free-breathing young children with congenital heart disease on cardiac 64-slice CT: dual-source ECG-triggered sequential scan vs. single-source non-ECG-synchronized spiral scan. *Pediatr Radiol* 2010;40:1670-1680
4. Goo HW. Current trends in cardiac CT in children. *Acta Radiol* 2013;54:1055-1062
5. Goo HW. Coronary artery imaging in children. *Korean J Radiol* 2015;16:239-250
6. Bang JH, Park JJ, Goo HW. Evaluation of commissural malalignment of aortic-pulmonary sinus using cardiac CT for arterial switch operation: comparison with transthoracic echocardiography. *Pediatr Radiol* 2017;47:556-564
7. Goo HW. Identification of coronary artery anatomy on dual-source cardiac computed tomography before arterial switch operation in newborns and young infants: comparison with transthoracic echocardiography. *Pediatr Radiol* 2018;48:176-185
8. Flohr TG, Leng S, Yu L, Aiimendinger T, Bruder H, Petersilka M, et al. Dual-source spiral CT with pitch up to 3.2 and 75 ms temporal resolution: image reconstruction and assessment of image quality. *Med Phys* 2009;36:5641-5653
9. Goetti R, Feuchtner G, Stolzmann P, Desbiolles L, Fischer MA, Karlo C, et al. High-pitch dual-source CT coronary angiography: systolic data acquisition at high heart rates. *Eur Radiol* 2010;20:2565-2571
10. Scharf M, Bink R, May MS, Hentschke C, Achenbach S, Uder M, et al. High-pitch thoracic CT with simultaneous assessment of coronary arteries: effect of heart rate and heart rate variability on image quality and diagnostic accuracy. *JACC Cardiovasc Imaging* 2011;4:602-609
11. Bamberg F, Marcus R, Sommer W, Schwarz F, Nikolaou K, Becker CR, et al. Diagnostic image quality of a comprehensive high-pitch dual-spiral cardiothoracic CT protocol in patients with undifferentiated acute chest pain. *Eur J Radiol* 2012;81:3697-3702
12. Kröpil P, Rojas CA, Ghoshhajra B, Lanzman RS, Miese FR, Scherer A, et al. Prospectively ECG-triggered high-pitch spiral acquisition for cardiac CT angiography in routine clinical practice: initial results. *J Thorac Imaging* 2012;27:194-201
13. Sun K, Han RJ, Ma LJ, Wang LJ, Li LG, Chen JH. Prospectively electrocardiogram-gated high-pitch spiral acquisition mode dual-source CT coronary angiography in patients with high heart rates: comparison with retrospective electrocardiogram-gated spiral acquisition mode. *Korean J Radiol* 2012;13:684-693
14. Bischoff B, Meinel FG, Del Prete A, Reiser MF, Becker HC. High-pitch coronary CT angiography in dual-source CT during free breathing vs. breath holding in patients with low heart rates. *Eur J Radiol* 2013;82:2217-2221
15. Wang Q, Qin J, He B, Zhou Y, Yang JJ, Hou XL, et al. Double prospectively ECG-triggered high-pitch spiral acquisition for CT coronary angiography: initial experience. *Clin Radiol*

2013;68:792-798
16. St Noble V, Douraghi-Zadeh D, Padley SP, Rubens MB, Nicol ED. Maximizing the clinical benefit of high-pitch, single-heartbeat CT coronary angiography in clinical practice. *Clin Radiol* 2014;69:674-677
17. Deseive S, Pugliese F, Meave A, Alexanderson E, Martinoff S, Hadamitzky M, et al. Image quality and radiation dose of a prospectively electrocardiography-triggered high-pitch data acquisition strategy for coronary CT angiography: the multicenter, randomized PROTECTION IV study. *J Cardiovasc Comput Tomogr* 2015;9:278-285
18. Lell MM, May M, Deak P, Alibek S, Kuefner M, Kuettner A, et al. High-pitch spiral computed tomography: effect on image quality and radiation dose in pediatric chest computed tomography. *Invest Radiol* 2011;46:116-123
19. Nie P, Wang X, Cheng Z, Ji X, Duan Y, Chen J. Accuracy, image quality and radiation dose comparison of high-pitch spiral and sequential acquisition on 128-slice dual-source CT angiography in children with congenital heart disease. *Eur Radiol* 2012;22:2057-2066
20. Zheng M, Zhao H, Xu J, Wu Y, Li J. Image quality of ultra-low-dose dual-source CT angiography using high-pitch spiral acquisition and iterative reconstruction in young children with congenital heart disease. *J Cardiovasc Comput Tomogr* 2013;7:376-382
21. Xu J, Zhao H, Wang X, Bai Y, Liu L, Liu Y, et al. Accuracy, image quality, and radiation dose of prospectively ECG-triggered high-pitch dual-source CT angiography in infants and children with complex coarctation of the aorta. *Acad Radiol* 2014;21:1248-1254
22. Nie P, Yang G, Wang X, Duan Y, Xu W, Li H, et al. Application of prospective ECG-gated high-pitch 128-slice dual-source CT angiography in the diagnosis of congenital extracardiac vascular anomalies in infants and children. *PLoS One* 2014;9:e115793
23. Sriharan M, Lazoura O, Pavitt CW, Castellano I, Owens CM, Rubens MB, et al. Evaluation of high-pitch ungated pediatric cardiovascular computed tomography for the assessment of cardiac structures in neonates. *J Thorac Imaging* 2016;31:177-182
24. Kanie Y, Sato S, Tada A, Kanazawa S. Image quality of coronary arteries on non-electrocardiography-gated high-pitch dual-source computed tomography in children with congenital heart disease. *Pediatr Cardiol* 2017;38:1393-1399
25. Goo HW. Individualized volume CT dose index determined by cross-sectional area and mean density of the body to achieve uniform image noise of contrast-enhanced pediatric chest CT obtained at variable kV levels and with combined tube current modulation. *Pediatr Radiol* 2011;41:839-847
26. Hui PKT, Goo HW, Du J, Ip JJK, Kanzaki S, Kim YJ, et al. Asian consortium on radiation dose of pediatric cardiac CT (ASCI-REDCARD). *Pediatr Radiol* 2017;47:899-910
27. Goo HW. CT radiation dose optimization and estimation: an update for radiologists. *Korean J Radiol* 2012;13:1-11
28. Beeres M, Wichmann JL, Frellesen C, Bucher AM, Albrecht M, Scholtz JE, et al. ECG-gated versus non-ECG-gated high-pitch dual-source CT for whole body CT angiography (CTA). *Acad Radiol* 2016;23:163-167
29. Wielandner A, Beitzke D, Schernthaner R, Wolf F, Langenberger C, Stadler A, et al. Is ECG triggering for motion artefact reduction in dual-source CT angiography of the ascending aorta still required with high-pitch scanning? The role of ECG-gating in high-pitch dual-source CT of the ascending aorta. *Br J Radiol* 2016 Jun 27 [Epub ahead of print]. https://doi.org/10.1259/bjr.20160174
30. Farshad-Amacker NA, Alkadhi H, Leschka S, Frauenfelder T. Effect of high-pitch dual-source CT to compensate motion artifacts: a phantom study. *Acad Radiol* 2013;20:1234-1239
31. Koch K, Oellig F, Oberholzer K, Bender P, Kunz P, Mildenberger P, et al. Assessment of right ventricular function by 16-detector-row CT: comparison with magnetic resonance imaging. *Eur Radiol* 2005;15:312-318
32. Goo HW, Park SH. Semiautomatic three-dimensional CT ventricular volumetry in patients with congenital heart disease: agreement between two methods with different user interaction. *Int J Cardiovasc Imaging* 2015;31 Suppl 2:223-232
33. Goo HW, Allmendinger T. Combined electrocardiography- and respiratory-triggered CT of the lung to reduce respiratory misregistration artifacts between imaging slabs in free-breathing children: initial experience. *Korean J Radiol* 2017;18:860-866
34. Beeres M, Loch M, Schulz B, Kerl M, Al-Butmeh F, Bodelle B, et al. Bolus timing in high-pitch CT angiography of the aorta. *Eur J Radiol* 2013;82:1028-1033
35. Beeres M, Williams K, Bauer RW, Scholtz J, Kaup M, Gruber-Rouh T, et al. First clinical evaluation of high-pitch dual-source computed tomographic angiography comparing automated tube potential selection with automated tube current modulation. *J Comput Assist Tomogr* 2015;39:624-628